The Astronomical Journal, 157:194 (11pp), 2019 May https://doi.org/10.3847/1538-3881/ab14f6

Total ALFALFA Neutral Hydrogen Fluxes for Extended Sources

G. Lyle Hoffman[1], Jayce Dowell[2], Martha P. Haynes[3], and Riccardo Giovanelli[3]
[1] Dept. of Physics, Lafayette College, Easton, PA 18042, USA; hoffmang@lafayette.edu
[2] Dept. of Physics and Astronomy, University of New Mexico, Albuquerque, NM 87131, USA
[3] Cornell Center for Astrophysics and Planetary Science, Space Sciences Building, Cornell University, Ithaca, NY 14853, USA
Received 2018 November 13; revised 2019 March 14; accepted 2019 March 30; published 2019 April 29

Abstract

A procedure is presented to improve on measurement of total H I fluxes for extended sources in the Arecibo Legacy Fast Arecibo *L*-band Feed Array (ALFALFA) survey of neutral hydrogen sources in the nearby universe. A number of tests of the procedure are detailed, and we verify that we recover all of the flux measured with much larger telescope beams. Total fluxes are reported for all sources (1) exceeding 10 Jy km s^{-1} in the α.100 catalog, or (2) with Uppsala General Catalog diameters 3.0 arcmin or more, or (3) ALFALFA pipeline isophotal ellipse area more than 3.0 times the Arecibo beam. Total fluxes are also provided for a number of confused pairs and small groups including one or more of those high-flux sources. These data should be of use in baryonic Tully–Fisher studies and other applications where the measurement of the total reservoir of neutral atomic gas is important.

Key words: galaxies: irregular – galaxies: spiral – intergalactic medium – radio lines: galaxies

Supporting material: machine-readable tables

1. Introduction

While the importance of the neutral hydrogen contents of galaxies as reservoirs of fuel for star formation has been recognized for a long time, the neutral hydrogen 21 cm spectral line fluxes have been notoriously difficult to measure precisely. Perusal of the fluxes reported in the NASA/IPAC Extragalactic Database (NED) for any galaxy of angular extent larger than a few arcminutes quickly reveals that the fluxes vary by as much as a factor of two, in many cases due to differences in calibration, in corrections for the size of the neutral hydrogen disk compared to the single-dish telescope beam, and in spectral baseline removal. Synthesis array mapping has also tended to underestimate the neutral hydrogen fluxes, due to the paucity of short baselines.

The Arecibo Legacy Fast ALFA (ALFALFA) survey (Giovanelli et al. 2005; Haynes et al. 2011) promises to improve H I flux measurements substantially. Its minimal intrusion design and careful attention to calibration against well-studied continuum sources along with its systematic, thorough mapping of all H I sources, its high sensitivity, and flat baselines in both spectral and time domains should produce galaxy fluxes on a more uniform scale than have previously been available. The pipeline procedures are optimized to produce accurate fluxes for unresolved sources and to produce high signal-to-noise ratio (S/N) measurements of profile widths and systemic redshifts, but the archived data include complete maps that make it possible to extract precise measurements of fluxes for resolved sources as well. The aim of the present paper is to develop a procedure for doing so.

The ALFALFA survey is described briefly in Section 2. Our procedure for measuring fluxes of resolved sources is outlined in Section 3. Results for the galaxies with H I emission of extent larger than the Arecibo beam follow in Section 4, and some details of interacting pairs and small groups that include one or more of those extended galaxies are added in Section 5. We finish with a summary in Section 6.

2. ALFALFA

The ALFALFA survey is described in detail by Haynes et al. (2018) and Giovanelli et al. (2005), so only the most pertinent details will be repeated here. The full catalog of external galaxies is presented in Haynes et al. (2018), hereafter referred to as α.100. The first 40% were presented by Haynes et al. (2011), hereafter referred to as α.40; the 70% survey (α.70) was made available online by Haynes (2016) and discussed by Jones et al. (2016).

ALFALFA is a drift-scan survey using the seven-beam Arecibo *L*-band Feed Array (ALFA). Observations were started in 2005 February and were completed in 2012 October. Reduction of the data is now complete. The full survey covers about 7000 deg^2 over a redshift range of about $-2000 < cz < 18{,}000$ km s^{-1} and has cataloged more than 30,000 galaxies. The final data products consist of "grids" or data cubes spanning $144 \times 144'$ on the sky and about 5300 km s^{-1} in cz (heliocentric). Four grids, coincident on the sky but at successive redshift intervals, are thus required to span the entire redshift range of the survey. For the lowest redshift grids relevant to most of the extended sources discussed here, the channel spacing is about 5.2 km s^{-1}, and pixels are $1'$ on a side. For a typical source integrated over the $3\farcm3 \times 3\farcm8$ beam, the rms noise in the spectrum is about 2.3 mJy. Diffuse emission can be recognized down to column densities of a few $\times 10^{18}$ cm^{-2}. Sources are identified by the three-dimensional matched-filtering procedure of Saintonge (2007), followed by interactive examination of the grids.

3. Prescription for Measuring Fluxes of Extended Sources

The ALFALFA pipeline procedure (GalFlux4.pro) for measuring hydrogen fluxes, systemic redshifts, and profile widths was optimized to give the most reliable profile widths and highest S/N measurements of total neutral hydrogen fluxes of unresolved sources (Haynes et al. 2011, 2018). In brief, the peak intensity pixel in a zeroth-moment map of a small region around a detected source is identified. An ellipse is drawn at the isophote at half the peak intensity, and the total flux density s_ν

Table 1
Total H I Fluxes for Galaxies with Large Angular Diameter

AGC	Name	R.A.(J2000) deg	Decl.(J2000) deg	cz km s^{-1}	UGC Diameter Arcmin	H I Size (dimensionless)	Total Flux Jy km s^{-1}	Flux Error Jy km s^{-1}	Pipeline Flux Jy km s^{-1}	Notes
12914	478-012	0.4092	23.4869	4342	2.7	1.5	15.17	0.28	10.06	*
12915	478-013	0.4146	23.4878	4378	1.6	1.5	15.17	0.28	11.39	*
8	NGC 7814	0.8100	16.1500	1050	6.5	2.4	18.94	0.21	22.08	*
17	…	0.9283	15.2183	876	3.0	1.3	6.16	0.12	6.70	
16	NGC 7816	0.9567	7.4836	5243	2.0	2.2	12.84	0.20	11.66	*
19	NGC 7817	1.0013	20.7519	2308	4.0	1.5	14.50	0.26	14.89	*
26	NGC 7819	1.1033	31.4706	4955	2.0	1.4	9.49	0.16	10.19	
27	408-020	1.1200	5.8447	3113	2.2	1.4	14.08	0.14	13.61	
57	NGC 1	1.8163	27.7139	4550	1.8	1.7	10.87	0.17	11.21	
75	NGC 14	2.1825	15.8142	855	3.0	2.5	18.58	0.10	17.99	

(This table is available in its entirety in machine-readable form.)

for each velocity channel, summed within that ellipse, is divided by the sum of a representation of the ALFA beam within the same ellipse, as in Equation (3) of Haynes et al. (2018):

$$S_\nu = \frac{\sum_x \sum_y s_\nu(\Delta x, \Delta y)}{\sum_x \sum_y B(\Delta x, \Delta y)} \text{ [mJy]}. \quad (1)$$

The H I flux $S_{\rm pipe} = \int s_\nu d\nu$ is just the sum over velocity channels. The beam B is taken to be an elliptical Gaussian with diameters 3.′8 by 3.′3. For the vast majority of the sources detected in the α.100 survey, this gives integrated flux densities in good agreement with those measured by telescopes with larger beams (Haynes et al. 2018). However, it underestimates the fluxes of sources that are significantly more extended than the Arecibo[4] beam, as determined by comparison with fluxes measured previously using the much larger beam of the Green Bank 140 Foot telescope[5] (Haynes et al. 1998).

To improve on these flux measurements for extended sources, we first extracted a rectangular grid a few pixels larger in each spatial dimension than the source appeared in any velocity channel. A spectrum was produced by integrating over the spatial map. From that preliminary spectrum, we identified the velocity channels that appear to contribute to the flux from the source, and we then reproduced the map integrated over just those velocity channels. On this map, we marked off a polygon enclosing those pixels within which the velocity-integrated flux exceeded the noise, at roughly 2σ. This was done by a human researcher with extensive experience with ALFALFA and other Arecibo observations. Due to the noise that varied across the map, the frequent presence of neighboring sources whose sidelobes overlapped those of the source to be measured, weak radio frequency interference (rfi) that was not excised in the primary data-reduction steps, and so on, algorithmic mask-making procedures could not be relied on. The same polygonal mask was applied to each velocity channel. Each decl. pixel within the polygon was scanned by a different combination of the seven beams that make up ALFA, and therefore was observed with a different effective beam (Irwin et al. 2009). As shown by the beam maps presented in Irwin et al. (2009), each of the outer feeds has significant coma lobes that contribute to pixels removed by as much as 12′ from the center of the feed. The flux value assigned to each point in the ALFALFA grids is determined by an average of the fluxes received in each of the seven feeds in two passes offset by 7′18″, weighted by a two-dimensional Gaussian in distance from the feed center. An effective beam is computed by simulating the observation of a theoretical point source at each decl., using the beam maps in Irwin et al. (2009) for the response of each feed. From the simulated drifts, the beam map is formed in the same manner as the grids themselves (Dowell 2010, J. D. Dowell et al. 2019, in preparation). Those effective beams for each of the decl. pixels in the polygon are then averaged over the covered declinations to produce a single average beam for the polygon. A spectrum over the entire frequency range of the grid is assembled from the pixels within the polygon, divided by the average beam centered on and integrated over the polygon as in Equation (1), and the total flux $S_{\rm poly}$ is found by integrating that spectrum between the velocity channels at which the feature of interest appears to reach the baseline. The uncertainty in that flux has contributions from the noise in the integrated-over portion of the grid, from the difference between the curvature of the fitted baseline in the spectrum and the unknown actual baseline under the H I feature, from unexcised rfi, and from calibration errors. We can estimate the first of those from the rms noise in the signal-free portions of the spatially integrated baseline, multiplied by the channel width in km s^{-1} and by the square root of the number of channels across the feature. That contribution is included in Table 1. The contributions due to baseline curvature, imperfectly determined beam structure, unrecognized rfi, and calibration errors are not so easy to quantify. We can obtain a rough estimate of the total error, excluding calibration errors, from the 36 examples of sources that were measured on two different occasions (using different polygons and in some cases in different grids) separated by a year or more. The difference between two such measurements is typically a few tenths of a Jy km s^{-1}, but averages to 1.29 Jy km s^{-1}, due to a few cases of strong sources with considerably larger differences. If we average percent differences instead, we obtain an average error of 3.9% (3.3% if one outlier is excluded from the average). For sources for which the H I distributions abut or overlap, so that judgment must be exercised in determining where to draw the boundary, the uncertainties are larger. The calibration of ALFALFA is

[4] The Arecibo Observatory is operated by SRI International under a cooperative agreement with the National Science Foundation (AST-1100968), and in alliance with Ana G. Mèndez-Universidad Metropolitana, and the Universities Space Research Association.

[5] The National Radio Astronomy Observatory is a facility of the National Science Foundation operated under cooperative agreement by Associated Universities, Inc.

thought to be better than other single-dish surveys, due to the many well-studied continuum sources encountered in the drift scans and the stability of the noise diodes in the ALFA feeds, as detailed in $\alpha.100$. However, the only means we have of estimating that contribution to the error budget is by comparison to other surveys, as discussed in the following subsection.

Our construction of the effective beam is not precise for the 16°–20° decl. swath, where the ALFALFA drift-scan mode had to be changed because of the proximity of the feed to zenith. Measured beam patterns for the required ALFA turret rotations in those drift scans are not available. However, the effective area of the beam should be nearly correct; the main difference amounts to a rotation of the effective beam with respect to the north–south axis on the sky. Averaged over the declinations within the polygon for any source, the spatial integral over the beam should differ by much less than the uncertainty in the integrated flux density.

More elaborate image segmentation analysis (e.g., Kass et al. 1988; Serra et al. 2015) might be appropriate for individual, well-resolved sources. However, it would only reduce the error due to the noise in each channel of the grid; errors due to baseline curvature, beam structure, rfi, and calibration would persist. Automation would be hampered by the need for human judgment to separate sources whose sidelobes overlap and by noise that is not uniform spatially; in practice, each velocity channel would have to be inspected for the appropriateness of the mask. This would add person-years to the endeavor, if applied to each of the more than 700 sources in Table 1.

3.1. Tests

Neutral hydrogen fluxes for sources measured with single beams are notoriously imprecise, due to uncertain corrections for incomplete coverage of the galaxy by the telescope beam, nonflat spectral baselines, and calibration errors. However, a sample of 104 isolated spiral galaxies with careful and high-S/N flux measurements using the Green Bank 140 Foot telescope (Haynes et al. 1998) can serve as flux standards. Due to the large size of the beam, corrections for source size should be negligible for the observed galaxies, and galaxies with known companions were excluded from the sample. Any H I-bearing companions in the 140 Foot beam that were not recognized before 1998 can be included within the polygon used for the ALFALFA comparison. In the $\alpha.40$ footprint, we have 13 sources in common with Haynes et al. (1998). The ratios of ALFALFA fluxes within encompassing polygons to those measured with the 140 Foot telescope average 0.989 ± 0.026 with a total range from 0.74 to 1.15. The standard deviation of the ratios is 0.094; if we assume, for want of a better argument, that the errors are equally distributed between the two systems, then the error in an individual measurement is about 7%.

For objects as extended as we consider here, synthesis arrays tend to underestimate total fluxes, due to the paucity of short baselines. One exception, for which a concerted effort was made to fill in the short baselines by combining data from two arrays, is the nearby dwarf irregular DDO 154 (Carignan & Purton 1998). Those authors obtained a total flux of 105 Jy km s^{-1}. From the ALFALFA data, the total flux enclosed in our polygon is 89.9 Jy km s^{-1}.

Six more objects, moderately extended beyond the Arecibo beam, were observed by Dowell (2010; see also J. D. Dowell et al. 2019, in preparation) with the Very Large Array. These galaxies were NGC 826a, UGC 4115, 4599, 5288, 5373, and 10014. For these, the ratio of ALFALFA flux within our polygons to the VLA flux averages to 1.06 ± 0.12, spanning the range 0.75–1.44.

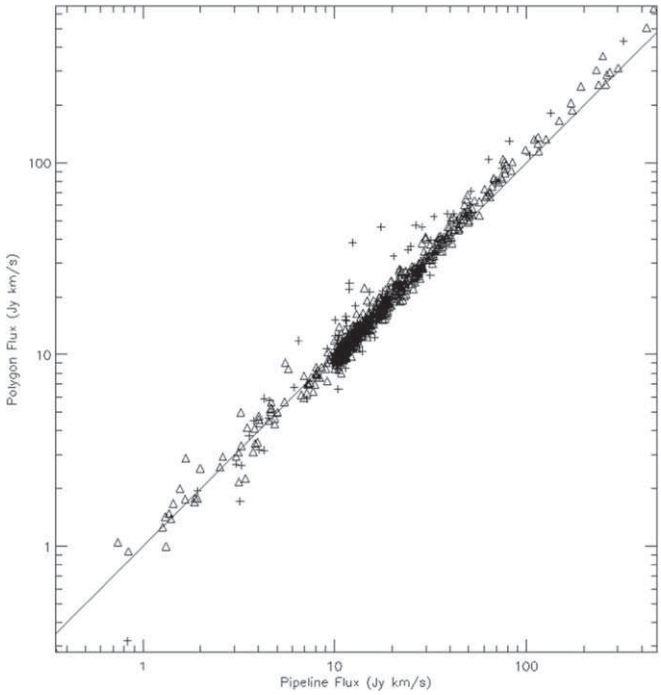

Figure 1. Flux measured within circumscribed polygons vs. $\alpha.100$ pipeline flux for all measured galaxies on logarithmic axes. Galaxies for which either polygon flux or pipeline flux is suspect due to rfi or confusion with other sources are plotted as plus signs (+), while all others are plotted as triangles. A line with unit slope is overplotted for reference. M33 is omitted.

4. Galaxies with Large Angular Extent

Since the ALFALFA pipeline procedures underestimate the fluxes of galaxies of large angular extent, we have remeasured the fluxes of strong H I sources from ALFALFA using our polygon procedure. We did so for all ALFALFA pipeline fluxes >10 Jy km s^{-1}. Linear regression gives $S_{\rm poly} = (-3.29 \pm 0.38) + (1.225 \pm 0.008)\ S_{\rm pipe}$, with both fluxes in Jy km s^{-1}. This would suggest that $S_{\rm poly} = S_{\rm pipe}$ at about 15 Jy km s^{-1}, as confirmed by Figures 1 (showing all measured galaxies) and 2 (zoomed in on pipeline fluxes less than 100 Jy km s^{-1}). M33 has been omitted from the comparison because ALFALFA did not report a flux for it. If the regression is restricted to pipeline fluxes $10 < S_{\rm pipe} < 20$ Jy km s^{-1}, we obtain $S_{\rm poly} = (-1.11 \pm 0.57) + (1.083 \pm 0.041)\ S_{\rm pipe}$, with both fluxes again in Jy km s^{-1}. The latter is not significantly different from a straight line with unit slope and zero intercept, confirming that the deviation of polygon fluxes from pipeline fluxes begins at a bit less than 20 Jy km s^{-1}. For sources in the $10 < S_{\rm pipe} < 20$ Jy km s^{-1} range, the rms difference between $S_{\rm poly}$ and $S_{\rm pipe}$ is about 0.6 Jy km s^{-1}, consistent with the uncertainty estimates quoted in the previous section.

Two other indicators of H I distribution size are available for most ALFALFA sources: the diameter of the optical counterpart and the size of the isophotal ellipse used to measure the ALFALFA pipeline fluxes. For the optical counterpart, we chose to use the diameters from the *Uppsala General Catalog of Galaxies* (UGC; Nilson 1972). The ALFALFA H I distributions for galaxies with UGC diameters of 3′ or larger

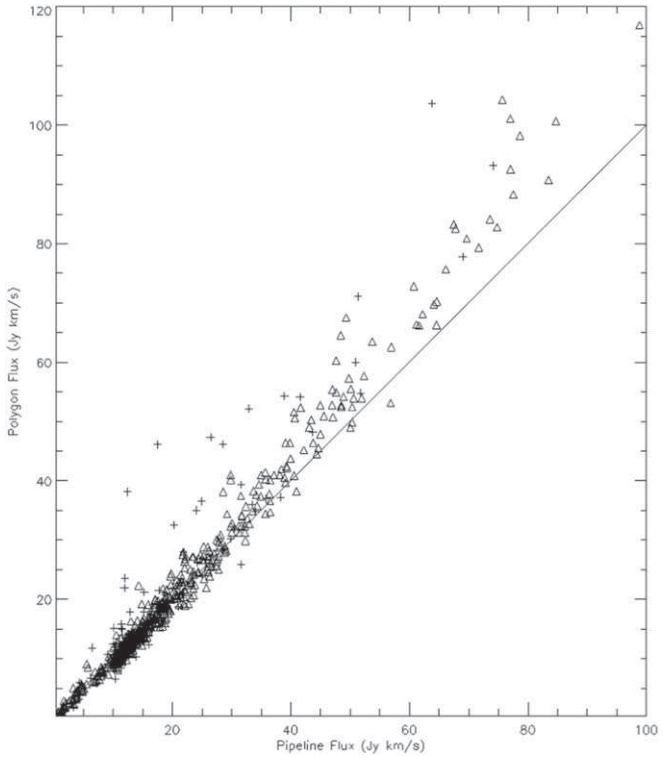

Figure 2. Flux measured within circumscribed polygons vs. $\alpha.100$ pipeline flux zoomed in on pipeline fluxes in the range 10–100 Jy km s^{-1} on linear axes. Galaxies for which either polygon flux or pipeline flux is suspect due to rfi or confusion with other sources are plotted as plus signs (+), while all others are plotted as triangles. A line with unit slope is overplotted for reference. M33 is omitted.

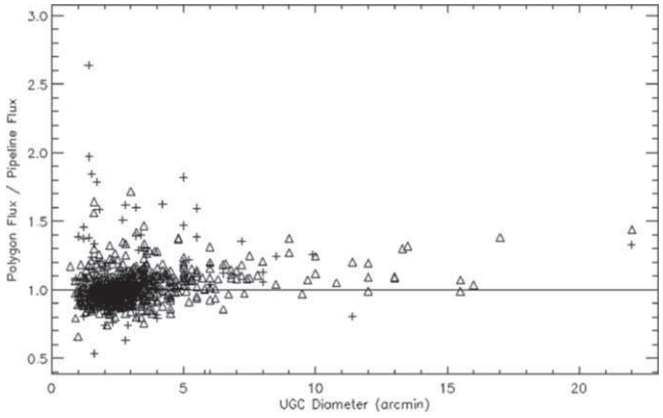

Figure 3. Ratio of polygon to pipeline fluxes as a function of UGC major diameter. The symbols are defined as for Figure 1. A line representing unity is overplotted for reference. M33 is omitted.

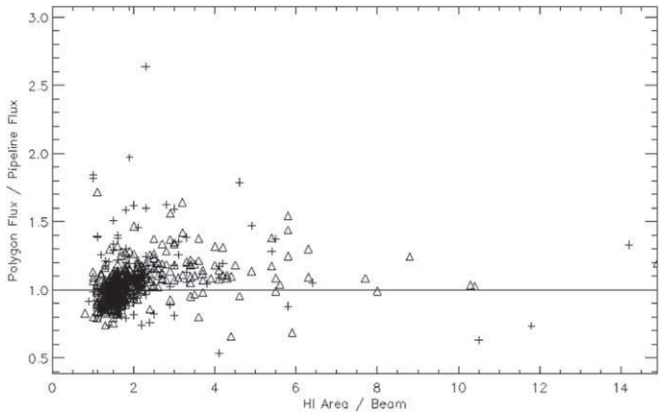

Figure 4. Ratio of polygon to pipeline fluxes as a function of the Hsize parameter (ratio of the pipeline isophotal ellipse area to the beam area). The symbols are defined as for Figure 1. A line representing unity is overplotted for reference. M33 is omitted.

were measured using our polygon procedure. Figure 3 displays the ratio of polygon flux to pipeline flux as a function of UGC diameter (including smaller diameters for galaxies with H I flux $S_{\rm pipe} > 10$ Jy km s^{-1}). The ratio trends greater than unity at UGC diameter about 4′. The large majority of these large-diameter galaxies also have large H I fluxes, but there are a few exceptions. The H I sizes of detected sources are encoded in the full ALFALFA database as the dimensionless parameter Hsize, defined to be the ratio of the area of the isophotal ellipse within which the spectrum is measured to the mean 3.′5 beam size: Hsize $= (a_{\rm ell}b_{\rm ell})/(3.'5)^2$. We completed polygon flux measurements for those with pipeline flux $S_{\rm pipe} \geqslant 3.0$ Jy km s^{-1} and Hsize $\geqslant 3.0$. Sources with smaller pipeline fluxes and large Hsize appear to have Hsize falsely inflated by noise. The ratio of polygon flux to pipeline flux as a function of Hsize is shown in Figure 4. The apparent shortfall of $S_{\rm poly}$ relative to $S_{\rm pipe}$ at the small-size end of the relation is probably due to the sidelobes of these weak sources being overwhelmed by noise. If our polygon is roughly the same size as the ellipse used in the ALFALFA pipeline with the outskirts of both being dominated by noise but our beam integral is larger, the polygon procedure produces a smaller flux estimate.

The total fluxes we measured are given in Table 1. A machine-readable version is available from the online edition of the Journal. The columns include (1) the galaxy's number in the AGC catalog (identical to the UGC number for those less than 13,000) and (2) an alternate name, either from the NGC/IC or Zwicky's CGCG; (3) and (4) the R.A. and decl. of the H I source from $\alpha.100$; (5) the heliocentric redshift, also from $\alpha.100$; (6) the UGC major diameter in arcmin; (7) the Hsize parameter (dimensionless); (8) the total flux $S_{\rm poly}$ integrated within our circumscribed polygon; (9) the contribution to the uncertainty in that flux due to noise in the grid (as explained above, the total error in each measurement is about 7%); and (10) the flux $S_{\rm pipe}$ for the central portion of the galaxy from $\alpha.100$. An asterisk in column (11) indicates that a note concerning that galaxy appears in the Appendix.

We refrain from reporting new values for each galaxy's redshift and profile width because the pipeline values of those quantities are measured at higher S/N and are more representative of the central disk of the galaxy. Only the total fluxes reported here should be taken in preference to the ALFALFA pipeline fluxes, when the total quantity of H I associated with the galaxy is required.

Previous flux measurements suffer from heterogeneous calibration, corrections for beam size, baseline uncertainties, and possible inclusion of companion galaxies in the reported values. The calibration of the ALFALFA survey is more homogeneous because it is tied to continuum sources in the same grids whose fluxes are presented in the Northern VLA Sky Survey (Condon et al. 1998). Baseline uncertainties persist, but should be small for these high-flux galaxies. Comparison to fluxes measured using other techniques in other surveys with Arecibo or other telescopes is a worthwhile sanity check, however. For each galaxy, we have selected the pre-

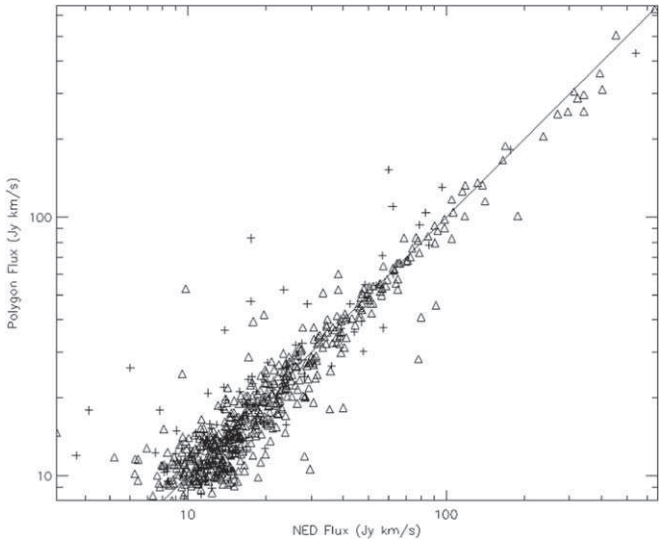

Figure 5. Flux measured within circumscribed polygons vs. flux from the NED archive, on logarithmic axes. The symbols are defined as in Figure 1. A line with unit slope is overplotted for reference. M33 is omitted.

ALFALFA measurement (as of summer 2018) most likely to account for the total flux of the galaxy with the smallest correction for beam coverage. In general, for galaxies of large angular extent, we have chosen larger beams; for galaxies that should be unresolved by more than one of the telescopes, we have chosen the more recent observations with more sensitive receivers by more experienced observers. We anticipate, and find, considerably more scatter in the correlation. The comparison is shown in Figure 5. Least-squares fitting gives $S_{\rm poly} = (2.04 \pm 0.47) + (0.910 \pm 0.007)\ S_{\rm NED}$, with both fluxes in Jy km s^{-1}. M33 has been omitted from this comparison as well, because its angular size greatly exceeds any of the beams used in previous measurements.

Table 2 presents the subset of polygon flux measurements that we consider to be preferred over α.100 pipeline fluxes for any purposes requiring the total H I reservoirs of galaxies. The entries in Table 2 include unconfused sources with pipeline flux $S_{\rm pipe} > 18$ Jy km s^{-1} or UGC diameter $a > 4'$; a few additional objects that fall below either of those limits, but have differences in polygon and pipeline fluxes that exceed our estimate of the polygon flux uncertainty and no indication of confusion with other sources, have been included as well. Columns (1) to (8) are the same as those for Table 1. Column (9) gives the distance $D_{\rm H}$ to the galaxy in Mpc from α.100, and column (10) reports the revised estimate of the H I mass $\log M_{\rm H}$ in units of the solar mass, calculated from the polygon flux $S_{\rm poly}$ and $D_{\rm H}$ by the standard formula $M_{\rm H} = 2.356 \times 10^5 D_{\rm H}{}^2 S_{\rm poly}$. An asterisk in Column (11) indicates that a note concerning that galaxy appears in the Appendix.

5. Interacting Pairs and Small Groups

Among the α.100 sources measured here, there are a number of tidally interacting pairs and small groups of galaxies and many more pairs that are close enough that their H I distributions are confused in the ALFALFA grids. Many of these have been studied in more detail, both with carefully chosen single-beam placements and with synthesis arrays. One contribution that ALFALFA can make that is difficult or uncertain from single-beam pointings or synthesis array mapping is the total H I flux of these systems. ALFALFA does not have the spatial resolution of the synthesis arrays, but it is sensitive to diffuse flux such as that from tidal tails.

Total fluxes for the 112 confused pairs and close groups are reported in Table 3 and in the notes to Table 1. The columns of Table 3 are (1) the AGC numbers of the member galaxies; (2) the total fluxes integrated over the combined area of the group; (3) the adopted distance, using the α.100 distance to the dominant member or α.100 distances weighted by the inverse squares of the uncertainties; and (4) the H I mass $\log M_{\rm H}$ in units of the solar mass for the group, calculated as for column (10) of Table 2. Further details about some notable examples follow.

NGC 871 (AGC 1759) and NGC 877 (AGC 1768) are members of an interacting quartet (Lee-Waddell et al. 2014). Two other members are NGC 876 (AGC 1766) and AGC 1761; AGC 748853 and AGC 749170 are involved as well. The emission from NGC 871 and NGC 877 each can be fairly well discriminated from the rest of the system. For the four galaxies as a group, along with tidal features, we measure 69.67 Jy km s^{-1}.

NGC 3020 and NGC 3024 (AGC 5271/5275) form a galaxy triple along with AGC 192239. The flux from each galaxy can be reasonably well discriminated. For the system of three galaxies, we measure 55.09 Jy km s^{-1}.

The Leo Triplet, consisting of AGC 6346/6350 (NGC 3627/3628) and NGC 3623 along with AGC 6395 (IC 2782), AGC 6401 (IC 2787), and a prominent tidal stream, has been studied extensively (Rots 1978; Haynes et al. 1979; Wilding et al. 1993; Stierwalt et al. 2009). Stierwalt et al. (2009) present a map of the H I in the group. We measure a flux of 371.59 Jy km s^{-1} for the system as a whole. For the tidal stream alone (excluding emission from the individual galaxies), we find 42.55 Jy km s^{-1}.

For the Leo Ring, AGC 205291 (Schneider 1985, 1989; Schneider et al. 1986, 1989; Stierwalt et al. 2009), we obtain a total flux of 57.17 Jy km s^{-1}. This is somwhat smaller than the 70 Jy km s^{-1} reported by Schneider (1989); it is unclear whether the difference is due to calibration differences or to different boundaries for the regions over which the flux was integrated.

The huge cloud around the NGC 4532/DDO 137 pair (AGC 7726/7739) was first reported by Hoffman et al. (1992, 1993, 1999), and ALFALFA (Koopmann et al. 2008) found that the H I tail extended much farther to the south. There is considerable ambiguity in distinguishing the flux of each galaxy from the other, but our measurement of 79.65 Jy km s^{-1} for the entire cloud (including both galaxies) is robust.

The triplet AGC 229196/229197/221639 constitutes H I 1225+01, the cloud complex in the southern extension of the Virgo cluster discovered serendipitously by Giovanelli & Haynes (1989) and mapped in more detail by Chengalur et al. (1995). Our total flux of 42.28 Jy km s^{-1} is about equal to the sum of the polygon fluxes of the three components, within the uncertainties. It exceeds the sum of fluxes from the synthesis array mapping (Chengalur et al. 1995) by about 20%, with most of the difference occurring in the northeast and bridge components.

Emission from NGC 7464/7465 (AGC 12315/12317) cannot be disentangled. The pair is in a quintet with NGC 7463 (AGC 12316), AGC 12313, and AGC 749072. The last

Table 2
H I Fluxes to Supercede ALFALFA Pipeline Fluxes

AGC	Name	R.A.(J2000) deg	Decl.(J2000) deg	cz km s^{-1}	UGC Diameter Arcmin	H I Size (dimensionless)	Total Flux Jy km s^{-1}	Distance Mpc	log $M_{\rm H}$ Solar Mass	Notes
8	NGC 7814	0.8100	16.1500	1050	6.5	2.4	18.94	13.2	8.89	*
191	434-001	5.0192	10.8822	1144	2.6	1.5	19.4	16.1	9.07	
231	NGC 100	6.0046	16.4889	842	5.8	2.2	44.49	18.4	9.55	
369	NGC 173	9.3029	1.9428	4366	4.0	1.7	22.98	60.9	10.30	
402	409-055	9.8296	3.9481	5291	1.6	3.2	9.08	74.1	10.07	
477	458-004	11.5517	19.4872	2647	3.5	1.7	27.78	35.2	9.91	
499	NGC 262	12.1975	31.9536	4540	1.6	2.9	22.32	65.9	10.36	*
668	IC 1613	16.2221	2.1269	−231	22.0	14.2	429.26	0.7	7.70	*
763	NGC 428	18.2346	0.9817	1151	5.0	2.5	83.31	11.3	9.4	
907	NGC 488	20.4442	5.2519	2270	6.0	2.5	19.8	30.8	9.65	*

(This table is available in its entirety in machine-readable form.)

Table 3
H I Fluxes for Blended Pairs and Groups

AGC Numbers	Total Group Flux Jy km s^{-1}	Distance Mpc	log $M_{\rm H}$ Solar Mass
12914/12915	15.17	61.9	10.14
19/101831	15.59	33.2	9.61
214/100740	13.65	75.7	10.27
260/100238	34.80	29.1	9.84
312/314/100286	21.51	53.7	10.16
484/100557	15.71	62.2	10.16
858/864	15.72	34.2	9.64
907/888/110254	21.13	32.0	9.71
966/957	40.04	29.3	9.91
1020/112333	15.78	33.8	9.63

(This table is available in its entirety in machine-readable form.)

three galaxies can be reasonably well separated from the blended pair, but some contamination of each is possible. A previous attempt to disentangle the emission from the various group members was made by Lu et al. (1993). For the quintet as a whole, we measure 82.57 Jy km s^{-1}.

6. Conclusions and Summary

This paper presents a procedure to obtain accurate fluxes for extended sources in the ALFALFA survey (Giovanelli et al. 2005; Haynes et al. 2011). With it, we are able to recover total H I fluxes for sources considerably larger than the $3\farcm3 \times 3\farcm8$ Arecibo beam, in agreement with those obtained in careful studies using telescopes of much larger beam size (Haynes et al. 1998). Total fluxes are reported for (1) all sources exceeding 10 Jy km s^{-1} in the complete ALFALFA extragalactic catalog, (2) additional galaxies with lower flux but with UGC major diameters $\geqslant 3\farcm0$ or with ratios of H I isophotal ellipse areas to the beam size $\geqslant 3$, and (3) a number of confused pairs and small groups including one or more of those sources. A subset of those sources for which the polygon fluxes are to be preferred over the $\alpha.100$ pipeline fluxes has been identified.

We thank M. Pinkard for assistance in testing the code and C. Giovanardi for helpful comments on an earlier draft of this paper. Perceptive comments from an anonymous referee have improved it. This research has made use of the NASA/IPAC Extragalactic Database (NED), which is operated by the Jet Propulsion Laboratory, California Institute of Technology, under contract with the National Aeronautics and Space Administration. Funding was provided through the Undergraduate ALFALFA Team from NSF grants AST-0724918, AST-0725267, AST-0725380, AST-0902211, AST-0903394, and AST-1637339, and by Lafayette College. Funding for the ALFALFA team at Cornell has been provided by NSF grants AST-0607007, AST-1107390, and AST-171428, and by grants from the Brinson Foundation.

Facility: Arecibo.

Software: IDL.

Appendix
Notes on Entries in Table 1

Notes concerning individual objects follow, in the order in which they appear in Table 1.

UGC 12914: Confused with UGC 12915; total flux is for the pair.
UGC 12915: Confused with UGC 12914; total flux is for the pair.
UGC 16: H I distribution extends past the north edge of the grid. Flux may be underestimated.
UGC 19: Total flux is for UGC 19 alone. For UGC 19 and AGC 101831 combined, the flux is 15.59 Jy km s^{-1}.
UGC 94: Near UGC 89, but there is minimal contamination.
AGC 100162: In a low-weight region of the grid; polygon cannot be drawn reliably.
AGC 100173: Undetected galaxy AGC 103156 falls within the measurement area.
UGC 214: Paired with AGC 100740 but separable. Combined flux is 13.65 Jy km s^{-1}.
UGC 260: Confused with AGC 100238; total flux is for the pair.
UGC 279: In a group with UGC 276 and AGC 100256, but there is minimal contamination.
UGC 312: Total flux is for the group of UGC 312, UGC 314, and nondetected AGC 100286.
UGC 356: UGC 354 and UGC 365 are nearby, but no overlap is evident.
UGC 365: Undetected galaxy AGC 100340 falls within the measurement area.
UGC 461: H I distribution may extend past the southern edge of the grid; total flux may be underestimated.
UGC 484: Confused with AGC 100557; total flux is for the pair.

UGC 499: Paired with AGC 102879; total flux includes an extension to the north.
UGC 597: Undetected galaxy UGC 592 falls within the measurement area.
UGC 624: In a group with UGC 623 and AGC 113996, but distinct.
UGC 668: H I distribution extends past the north edge of the grid. Flux is underestimated.
UGC 685: Spectral feature is adjacent to Galactic H I but does not overlap it.
UGC 852: The galaxy falls within a region of low weight in the grid. Measurement polygon cannot be drawn reliably.
UGC 858: Confused with UGC 864. Total flux is for the pair.
UGC 864: Confused with UGC 858.
AGC 110254: Nothing evident at that position.
UGC 907: In group with AGC 110254 and UGC 888, but could be reasonably separated. Total flux for the group of UGC 907, UGC 888, and AGC 110254 is 21.13 Jy km s^{-1}.
UGC 914: Radio frequency interference wipes out the low-velocity edge of the profile. Flux is underestimated.
UGC 966: Total flux is for the pair UGC 966 and UGC 957. If the extension to the southeast is included, the total flux is 40.04 Jy km s^{-1}.
UGC 1020: Confused with AGC 112333.
UGC 1065: Confused with UGC 1064 and AGC 111935.
UGC 1177: Paired with UGC 1172, but there is no confusion.
UGC 1197: In a low-weight region of the grid.
UGC 1205: Minimally confused with AGC 111168; total flux for the pair is 15.32 Jy km s^{-1}.
UGC 1248: S/N is too low for measurement polygon to be drawn.
UGC 1249: Adjacent to UGC 1256; some contamination is possible.
UGC 1256: Adjacent to UGC 1249; some contamination is possible. For the pair we obtain a total flux of 272.34 Jy km s^{-1}.
UGC 1269: Total flux is for the pair UGC 1269 and UGC 1272. Nondetected galaxies AGC 110538 and AGC 110541 are also in the measurement area.
UGC 1280: Confused with UGC 1286; total flux for the pair is 16.70 Jy km s^{-1}. Undetected galaxy AGC 110547 falls within the measurement polygon.
UGC 1292: Minimally confused with AGC 111210.
UGC 1305: In a group with UGC 1286, UGC 1280, UGC 1310, UGC 1313, and nondetected AGC 110547, but minimally confused. Total flux for the group is 48.51 Jy km s^{-1}.
UGC 1313: Near edge of grid; flux may be underestimated slightly. Confused with UGC 1310, but a reasonable attempt to separate the two fluxes was possible. The flux for the pair is 25.47 Jy km s^{-1}.
UGC 1382: Minimal confusion with AGC 411154. Near south edge of grid; flux may be underestimated.
UGC 1444: Paired with AGC 110684, but there is no confusion.
UGC 1446: Possible confusion with AGC 111368; total flux for the pair is 17.14 Jy km s^{-1}.
UGC 1466: Possible confusion with UGC 1463; total flux for the pair is 92.42 Jy km s^{-1}.
UGC 1556: Undetected galaxy UGC 1555 falls within the measurement area.
UGC 1581: In a group with undetected AGC 120016 and AGC 120019.
UGC 1643: Undetected galaxy AGC 121208 falls within the measurement area.
UGC 1678: Paired with UGC 1680; total flux for the pair is 17.67 Jy km s^{-1}.
AGC 121503: Paired with UGC 1739; total flux for the pair is 14.74 Jy km s^{-1}.
UGC 1759: Member of an interacting system with UGC 1761, 1766, and 1768, but the flux due to UGC 1759 can be separated out by velocity.
UGC 1766: Confused with UGC 1759, 1761, 1768, AGC 748853, and AGC 749170. The tabulated flux is our best estimate for UGC 1766 alone; for the system, we measure 69.67 Jy km s^{-1}
UGC 1768: Member of an interacting system with UGC 1759, 1761, and 1766, AGC 748853, and AGC 749170. Polygon excludes most of the flux from the other galaxies, but there may be some contamination. The total flux for the system is 69.67 Jy km s^{-1}.
UGC 1833: Confused with UGC 1828.
UGC 1937: Confused with UGC 1936.
UGC 2048: Confused with UGC 2047 and nondetected AGC 121426.
UGC 2049: Confused with UGC 2039.
UGC 2059: Possible intrinsic absorption.
UGC 2103: Nondetected AGC 120383 is in the area.
UGC 2140: Nondetected galaxies AGC 120404, AGC 120407, and AGC 121407 are in the area; in portion of grid with low weight.
UGC 2156: Near AGC 120429, but there is minimal confusion.
UGC 2188: The nondetected galaxy AGC 122713 is in the polygon.
UGC 2302: Near the north edge of the grid; flux may be underestimated.
AGC 122708: Undetected galaxies AGC 122709 and AGC 122710 fall within the measurement area.
UGC 2487: Confused with AGC 131430, AGC 131431, AGC 131432, AGC 131433, AGC 131434, and AGC 131435.
AGC 170209: Total flux is for AGC 170209 and AGC 170418 combined. UGC 3925 is also in the group; the total flux for all is 11.17 Jy km s^{-1}.
UGC 4005: Confused with AGC 170226.
UGC 4054: At southern edge of grid; flux may be underestimated.
UGC 4315: Nondetected AGC 180175 is in the area.
UGC 4366: Nondetected AGC 182130 is in the area.
UGC 4469: Nondetected AGC 180348 is in the area.
UGC 4541: Confused with AGC 180447; flux is for the pair. Undetected galaxy AGC 734141 falls within the measurement area.
UGC 4691: Possible confusion with AGC 182217; total flux for the pair is 11.41 Jy km s^{-1}.
UGC 4744: Paired with AGC 193999, but no confusion is evident.
UGC 4820: Galaxies UGC 4823 and AGC 190795 are nearby, but do not appear to be confused with UGC 4820.
UGC 5001: Nearby galaxy UGC 5004 does not appear to be confused with UGC 5001.

UGC 5092: Confused with UGC 5096; polygon flux is for the pair. UGC 5093 is also nearby; for the triple, we measure 6.20 Jy km s^{-1}. Undetected galaxies AGC 190815 and 193808 also fall within the measurement area.
UGC 5099: Confused with AGC 193671. Flux measurement is for the pair.
AGC 198305: Overlaps Galactic H I; median sky was removed. Flux is uncertain.
UGC 5140: Nondetected AGC 195354 is in the area.
UGC 5167: AGC 192833 is nearby, but remains distinct.
UGC 5183: Possible confusion with UGC 5190 and AGC 194074. Total flux for the group is 26.00 Jy km s^{-1}.
UGC 5228: Undetected AGC 191806 lies in the polygon.
UGC 5229: Confused with AGC 190767 and nondetected AGC 190870.
UGC 5230: Grouped with AGC 191323 and nondetected galaxies AGC 190492 and AGC 733851; total flux for the group is 41.71 Jy km s^{-1}.
UGC 5248: Near AGC 190953, but confusion is minimal.
UGC 5265: Flux could not be separated from that for UGC 5269.
UGC 5269: Confused with UGC 5265; polygon flux measurement is for the pair along with the undetected AGC 191599.
UGC 5271: Member of a triple including UGC 5275 and AGC 192239. Polygon mostly excludes the other two galaxies, but some contamination is possible. Total flux for the system is 55.09 Jy km s^{-1}.
UGC 5272: Nondetected AGC 191701 is in the area.
UGC 5275: Member of a triple including UGC 5271 and AGC 192239. Polygon mostly excludes the other two galaxies, but some contamination is possible.
UGC 5325: Nondetected AGC 731174 is in the area.
AGC 192281: Measurement area contains undetected galaxies AGC 190317, 190644, 190645, 192271, 193990, and 193991.
UGC 5364: May be some contamination from Galactic H I.
UGC 5366: Confused with AGC 205868.
UGC 5452: Paired with UGC 5446. Total flux for the pair is 26.33 Jy km s^{-1}.
UGC 5470: S/N is too low for a flux measurement polygon to be drawn.
UGC 5473: Confused with AGC 205355; flux measurement is for the pair.
UGC 5495: Nondetected AGC 739232 is in the area.
UGC 5510: Possible confusion with AGC 200162.
UGC 5516: Cannot be distinguished from UGC 5525. UGC 5512, AGC 208457, and AGC 208534 are also in the vicinity.
UGC 5525: Flux is contaminated by AGC 208534 and AGC 208457, which together contribute about 11.15 Jy km s^{-1}. UGC 5516 cannot be distinguished from UGC 5525, and UGC 5512 is also in the area.
AGC 208538: Confused with AGC 208329 and AGC 208539; flux is for the triplet. AGC 204288 is also nearby, but distinct.
UGC 5556: Grouped with UGC 5559 and UGC 5562. Total flux for the group is 14.48 Jy km s^{-1}.
UGC 5559: Some contamination from UGC 5562 and UGC 5556 may persist.
UGC 5561: Confused with AGC 200241 and AGC 203459. Total flux for the group is 15.28 Jy km s^{-1}.
UGC 5601: Nondetected galaxies AGC 201038, AGC 208704, AGC 739321, and AGC 739334 all lie in or near the measurement area.
AGC 202046: May be confused with AGC 208716 and AGC 208744; total flux for the triplet is 4.22 Jy km s^{-1}. AGC 208745 is also nearby but appears distinct.
UGC 5620: Grouped with UGC 5617, AGC 208715, and nondetected AGC 739353. Total flux is for the group.
UGC 5711: Grouped with nondetected galaxies AGC 722272 and AGC 200442.
UGC 5852: Paired with nondetected galaxy AGC 208494.
UGC 5878: Nondetected AGC 201090 lies within the measurement area.
UGC 5931: Paired with UGC 5935 and in group with UGC 5927 and AGC 201947. Total flux is for the pair; if UGC 5927 and AGC 201947 are included, the total flux rises to 60.27 Jy km s^{-1}.
UGC 5965: Confused with UGC 5964. Total flux for the pair is 12.46 Jy km s^{-1}.
UGC 5972: Probable contamination from UGC 5982.
UGC 5980: Grouped with AGC 204427 and AGC 204429, but minimal confusion.
UGC 5982: Grouped with UGC 5972 and AGC 201948. Total flux for the group is 60.31 Jy km s^{-1}.
UGC 6006: Nondetected UGC 6007 and AGC 740242 lie within the measurement area.
UGC 6028: Nondetected UGC 6026 lies within the measurement area.
UGC 6116: Near UGC 6123, but there is minimal overlap in the H I distributions.
UGC 6123: Interacting with UGC 6118, but flux could be separated reasonably well.
UGC 6134: Grouped with AGC 214183, AGC 214186, and AGC 215457, all nondetected.
UGC 6150: Near edge of grid; flux may be underestimated slightly.
UGC 6200: Near edge of grid; flux may be underestimated.
UGC 6272: Nondetected AGC 215387 is in the area.
UGC 6305: Confused with UGC 6306.
UGC 6346: Member of the Leo Triplet. Flux is reasonably well confined to UGC 6346 alone.
UGC 6350: Dominant member of the Leo Triplet. This flux is for UGC 6350 alone, excluding UGC 6346 and the tidal stream. For the entire system (UGC 6346, UGC 6350, UGC 6395, UGC 6401, and the tidal stream that incorporates AGC 215414, 215413, and 215412), we obtain a total flux of 371.59 Jy km s^{-1}. For the tidal stream alone (excluding UGC 6350), we have 42.55 Jy km s^{-1}.
UGC 6376: Nondetected AGC 740789 lies within the measurement area.
UGC 6419: UGC 6418 and nondetected AGC 210303 are in close proximity. The flux for UGC 6419 could be separated reasonably cleanly. The flux for the system of three galaxies is 25.08 Jy km s^{-1}.
UGC 6445: May be interacting with UGC 6453, but fluxes could be separated cleanly.
UGC 6453: May be interacting with UGC 6445, but fluxes could be separated cleanly.
UGC 6479: Grouped with AGC 210362, AGC 210363, AGC 212245, AGC 212701, and AGC 741001, all nondetected.

UGC 6536: Grouped with nondetected AGC 723722 and AGC 723772. AGC 749437 is also nearby, but its H I distribution is distinct.
UGC 6586: Grouped with UGC 6588, for which the H I distribution is distinct, and nondetected AGC 211692.
UGC 6614: Grouped with AGC 210563, AGC 741221, and AGC 741225, all nondetected.
UGC 6623: Confused with UGC 6621. Total flux is for the pair.
UGC 6692: Possible confusion with AGC 210665.
UGC 6693: Paired with nondetected AGC 719483.
UGC 6722: In a low-weight portion of the grid.
UGC 6754: Minimally confused with AGC 741402. Total flux for the pair is 9.74 Jy km s^{-1}.
UGC 6772: Paired with nondetected AGC 724058.
UGC 6784: Paired with nondetected AGC 747800.
UGC 6786: Paired with nondetected AGC 211871.
UGC 6803: Paired with AGC 731805, but the H I distributions are distinct.
UGC 6806: Total flux is for the pair UGC 6806 and UGC 6807.
UGC 6807: Total flux is for the pair UGC 6806 and UGC 6807.
UGC 6933: Grouped with UGC 6936, UGC 6944, and nondetected AGC 212393; total flux is for the group.
UGC 6944: Grouped with UGC 6933, UGC 6936, and nondetected AGC 212393; total flux is for the group.
UGC 6954: Adjacent to UGC 6967, which may contaminate this spectrum.
UGC 6967: Adjacent to UGC 6954, which may contaminate this spectrum slightly. UGC 6954 and UGC 6967 combined produce a flux of 33.2 Jy km s^{-1}.
UGC 6968: Undetected galaxies AGC 210396, 210957, 724291, 724303, 724305, 724306, 724307, 724308, and 724309 are nearby.
UGC 7001: Flux excludes much weaker adjacent source AGC 211006. For the pair as a whole, we obtain a flux of 14.61 Jy km s^{-1}.
UGC 7012: Grouped with UGC 7017 and AGC 212371. Total flux for the pair UGC 7012 and UGC 7017 is 16.19 Jy km s^{-1}, and that for the triplet is 17.25 Jy km s^{-1}.
UGC 7111: Interacting with UGC 7116, but there is little overlap of the fluxes. Nondetected AGC 224238 is also within the measurement area.
UGC 7130: Grouped with AGC 220142 and AGC 220144; total flux for the group is 23.60 Jy km s^{-1}.
UGC 7143: Paired with nondetected AGC 731973.
UGC 7193: Confused with AGC 221647. Polygon flux is for the pair.
UGC 7225: Near AGC 724592, but there is minimal confusion.
UGC 7231: Feature straddles Galactic H I, which has been interpolated over. Uncertainty is considerably larger than for most other entries.
UGC 7256: Total flux includes very weak AGC 226633.
UGC 7261: Nondetected AGC 742131 is within the measurement area.
UGC 7275: Feature straddles Galactic H I, which has been interpolated over. The flux has higher uncertainty than most entries.
UGC 7284: Galactic H I has been edited out of the feature. The flux has higher uncertainty as a result.
UGC 7291: Grouped with UGC 7284 and AGC 220256. Total flux for the group is 36.56 Jy km s^{-1}.
UGC 7386: Paired with UGC 7398, which may contaminate this spectrum. The total flux for the pair is 11.58 Jy km s^{-1}.
UGC 7405: Very low S/N; measurement polygon is quite uncertain.
UGC 7407: Paired with UGC 7414, which may contaminate this spectrum. For the pair as a whole, we measure 45.92 Jy km s^{-1}.
UGC 7414: Paired with UGC 7407, which may contaminate this spectrum.
UGC 7420: Nearby galaxy UGC 7439 is distinct in velocity and is not confused with this spectrum.
UGC 7439: Nearby galaxy UGC 7420 is distinct in velocity and is not confused with this spectrum.
UGC 7442: May overlap Galactic H I; flux is underestimated.
UGC 7445: Undetected galaxy AGC 221722 falls within the measurement area.
UGC 7497: Paired with AGC 220546, but the H I distributions are distinct.
UGC 7505: AGC 749236 is 10′.NE, but there is no significant contamination of this spectrum.
UGC 7520: Undetected galaxy AGC 224745 falls within the measurement area.
UGC 7526: High-velocity edge of the spectrum is confused with Galactic H I. The flux uncertainty is larger than most entries.
UGC 7537: Adjacent to UGC 7546, which may contaminate this spectrum. Total flux for the pair is 25.71 Jy km s^{-1}.
UGC 7546: Adjacent to UGC 7537, which may contaminate this spectrum.
UGC 7561: Polygon flux includes an extended tail to the southeast.
AGC 229196: Grouped with AGC 229197 and AGC 221639, but appears separable.
AGC 229197: Near AGC 221639 and AGC 229196, but appears to be distinct.
AGC 221639: Triple system with AGC 229196 and AGC 229197. Total flux for the triplet is 42.28 Jy km s^{-1}.
UGC 7663: Nondetected AGC 227308 is in the area.
UGC 7718: S/N is too low for a measurement polygon to be drawn.
UGC 7726: Paired with UGC 7739, and the two are surrounded by an extended common envelope of H I. The tabulated measurement is for UGC 7726 alone, but with some uncertainty about where to separate it from UGC 7739 and the extended cloud. For the pair, we obtain 71.28 Jy km s^{-1}, and if the extension to the southwest is included, the flux rises to 79.65 Jy km s^{-1}.
UGC 7739: Paired with UGC 7726, and the two are surrounded by a common envelope of H I. This measurement is for UGC 7739 alone, as best as we can separate it from UGC 7726.
UGC 7786: High-velocity edge confused with Galactic H I; total flux is uncertain.
UGC 7808: Near AGC 222533, but there does not appear to be any confusion.
UGC 7843: Low-velocity edge of the spectrum is lost to rfi; flux is underestimated.
UGC 7852: Grouped with UGC 7851 and AGC 220926, both nondetected.
UGC 7865: Total flux includes extension to the southeast.

UGC 7870: Near southern edge of grid; flux may be underestimated.
UGC 7874: Confused with UGC 7875; total flux is for the pair. Low-velocity edge is confused with Galactic H I.
UGC 7907: Flux integration area includes nondetected AGC 220979. For the group consisting of UGC 7907, UGC 7865, UGC 7860, AGC 220979, AGC 229488, 229489, and AGC 747978, the total flux is 1022.79 Jy km s^{-1}.
UGC 7969: Paired with AGC 221026 but separable; total flux for the pair is 8.54 Jy km s^{-1}.
UGC 7980: Low-velocity edge of the spectrum is poorly defined.
AGC 728364: Undetected galaxies AGC 728353, 728357, and 748000 fall within the measurement area.
UGC 8005: Total flux includes the extension AGC 229104.
AGC 229104: This object is an extension of UGC 8005; the total flux is for UGC 8005 plus the extension.
UGC 8033: Nondetected AGC 226010 is within measurement area.
UGC 8098: Flux integration area includes nondetected AGC 221619 and AGC 226728.
UGC 8155: Total flux may include contamination from AGC 238802.
UGC 8221: Paired with nondetected AGC 234315.
UGC 8248: Paired with nondetected AGC 742793.
UGC 8261: Paired with UGC 8280. Total flux for the pair is 19.29 Jy km s^{-1}.
UGC 8318: Flux integration area includes nondetected AGC 728758.
UGC 8475: Grouped with UGC 8486 (distinct H I distribution) and nondetected AGC 232223 and AGC 232290.
UGC 8559: Paired with UGC 8558 but distinct; undetected galaxies AGC 231775, 713521, 713523, and 713529 are within the measurement area.
UGC 8560: Grouped with UGC 8548 (minimal confusion) and nondetected AGC 234908. Total flux for the group is 18.64 Jy km s^{-1}.
UGC 8566: Minimally confused with AGC 238959. Total flux for the pair is 11.76 Jy km s^{-1}.
UGC 8573: Grouped with UGC 8558 and AGC 231050 (minimally confused) and with nondetected AGC 713525, AGC 713527, and AGC 713541. Total flux for the group is 15.98 Jy km s^{-1}.
UGC 8645: Confused with UGC 8641 and nondetected AGC 239015.
UGC 8739: Grouped with nondetected AGC 235286 and AGC 729270.
UGC 8787: Minimally confused with AGC 233264. Nondetected AGC 231536 is also in the group.
UGC 8831: UGC 8821 and AGC 232141 are in the vicinity, but appear distinct.
UGC 8847: Near the outskirts of UGC 8853 and near AGC 232143, but distinct.
UGC 8856: Undetected galaxy AGC 231615 is within the measurement area.
UGC 8865: Grouped with AGC 238888 (minimal confusion) and nondetected AGC 232134.
UGC 8902: Confused with AGC 230893. Polygon flux is for the pair.
UGC 8963: Grouped with UGC 8955, AGC 241333, and AGC 245335 (all nondetected).
UGC 8967: Grouped with UGC 8958 (minimal confusion) and nondetected AGC 240011 and AGC 240016.
UGC 8973: Confused with UGC 8972.
UGC 8987: Undetected galaxy AGC 21373 is within the measurement area.
UGC 9002: Paired with nondetected AGC 240060.
UGC 9031: Undetected galaxy AGC 735681 is within the measurement area.
UGC 9037: Paired with AGC 243959, but the H I distributions are distinct.
UGC 9061: Total flux may incorporate AGC 240141; nondetected galaxies AGC 744044 and AGC 744063 are also in the area.
UGC 9164: Paired with nondetected AGC 744315.
UGC 9172: Grouped with UGC 9175 and UGC 9176. Contamination or excluded flux may be possible.
UGC 9175: Grouped with UGC 9172 and UGC 9176. The total flux for the triplet is 24.98 Jy km s^{-1}.
UGC 9182: Paired with AGC 744380, but the H I distributions are distinct.
UGC 9183: Paired with UGC 9181, but the H I distributions are distinct.
UGC 9249: Paired with nondetected AGC 244328.
UGC 9254: Grouped with AGC 240381, AGC 243427, and AGC 243433, but confusion is minimal.
UGC 9283: Grouped with AGC 240384, AGC 240393, AGC 240397, AGC 240406, and AGC 726598, but there is no evident confusion. High-order polynomial was required to fit baseline.
UGC 9334: Paired with nondetected AGC 244450.
UGC 9346: This measurement excludes flux from the much smaller adjacent galaxy, UGC 9345. For the pair, we obtain 26.5 Jy km s^{-1}.
UGC 9356: Paired with AGC 241275. Total flux for the pair is 20.08 Jy km s^{-1}.
UGC 9465: Paired with AGC 245246, but the H I distributions appear distinct. Total flux for the pair is 17.53 Jy km s^{-1}.
UGC 9483: Paired with UGC 9485. Total flux for the pair is 22.49 Jy km s^{-1}.
UGC 9537: Radio frequency interference in the spectral feature was interpolated over.
AGC 249265: Undetected galaxy AGC 249276 falls within the measurement area.
UGC 9574: Nondetected UGC 9573 is within measurement area.
UGC 9576: Blended with UGC 9579; fluxes could not be separated.
UGC 9579: Blended with UGC 9576; flux is for the pair.
UGC 9728: Confused with UGC 9724 and nondetected AGC 746197.
UGC 9760: Grouped with AGC 252534, AGC 253656, and AGC 253667 (all nondetected).
UGC 9910: Paired with UGC 9918, but the H I distributions appear distinct.
UGC 9918: Paired with UGC 9910, but the H I distributions appear distinct.
UGC 9962: In a region of low weight; polygon cannot be drawn reliably.
UGC 10033: Nondetected galaxies AGC 251603 and 747080 are within the measurement area.

UGC 10288: The H I distribution overlaps the southern edge of the southermost grid; polygon flux cannot be measured.
UGC 10363: Confused with AGC 268008. Polygon flux is for the pair.
UGC 11830: At edge of grid; may be missing some flux.
UGC 11844: Minimally confused with UGC 11845. Total flux for the pair is 16.29 Jy km s^{-1}.
UGC 11859: Paired with AGC 311140, but confusion is minimal.
UGC 11866: Paired with AGC 310467, but confusion is minimal.
UGC 11910: Coincident with undetected galaxy AGC 320905; low S/N.
UGC 11968: Blended with UGC 11964.
UGC 11984: Confused with UGC 11985 and minimally with AGC 321502.
UGC 12018: Confused with AGC 321456; total flux for the pair is 16.07 Jy km s^{-1}. Minimally confused with UGC 12011 and 320556; AGC 320841 is also in the group but remains distinct.
AGC 320196: Nondetected AGC 320193 is in the area.
UGC 12193: Confused with UGC 12191 and nondetected AGC 320382.
UGC 12281: Grouped with AGC 320881, AGC 321187, and AGC 321191. Total flux for the group is 32.24 Jy km s^{-1}.
AGC 749072: Confused with UGC 12316.
UGC 12313: Adjacent to UGC 12317/12315; may include some contamination from those galaxies, as well as from UGC 12316.
UGC 12316: Adjacent to UGC 12317/12315 and AGC 749072, any of which may contaminate this spectrum.
UGC 12317: Blended with UGC 12315 and adjacent to UGC 12316 and UGC 12313, which may contaminate this spectrum. For the entire group (UGC 12313, 12315, 12316, 12317, and AGC 749072) we obtain 82.57 Jy km s^{-1}.
UGC 12343: At north edge of grid; total flux is a lower limit.
UGC 12344: Grouped with UGC 12347 and UGC 12351. Total flux for the group is 32.66 Jy km s^{-1}.
UGC 12378: Paired, but minimally confused, with UGC 12365. Total flux for the pair is 14.09 Jy km s^{-1}.
UGC 12391: Paired with nondetected AGC 330074.
UGC 12423: UGC 12426 is adjacent, but does not contaminate the flux measurement.
UGC 12430: Somewhat confused with UGC 12427. Total flux for the pair is 20.70 Jy km s^{-1}.
UGC 12437: Grouped with UGC 12438 (minimal confusion) and nondetected AGC 332492. Total flux for the triplet is 18.06 Jy km s^{-1}.
UGC 12447: Confused with UGC 12442. Total flux for the pair is 54.33 Jy km s^{-1}.
UGC 12486: Nondetected AGC 331572 is within the measurement area.
AGC 330245: Near AGC 330241 but separable; undetected AGC 330252 is also nearby.
UGC 12542: Low-velocity edge of the spectrum may be confused with UGC 12544.
UGC 12578: Near edge of grid; total flux is a lower limit.
UGC 12613: Galactic H I is sufficiently displaced from the feature that there is no confusion.
UGC 12639: Minimally confused with AGC 333401.
UGC 12660: Minimally confused with UGC 12662. Total flux for the pair is 16.83 Jy km s^{-1}.
UGC 12682: Total flux is uncertain; may be confused with UGC 12681. For the pair we measure 30.50 Jy km s^{-1}.
UGC 12681: Total flux is uncertain; may be confused with UGC 12682. For the pair we measure 30.50 Jy km s^{-1}.
UGC 12700: Blended with UGC 12699.
UGC 12707: Possible confusion with AGC 331623.
UGC 12737: Blended with UGC 12738; total flux is for the pair.
UGC 12738: Blended with UGC 12737; total flux is for the pair.
UGC 12788: Minimally confused with AGC 330937.
UGC 12815: Grouped with UGC 12808, UGC 12813, AGC 331745, AGC 331746, AGC 331747, AGC 332131, and AGC 332132. Total flux for the group is 22.62 Jy km s^{-1}.
UGC 12834: Grouped with UGC 12827, UGC 12831, UGC 12833, and AGC 330995 but minimally confused. Total flux for the group is 19.84 Jy km s^{-1}.
UGC 12846: Total flux may be missing the southern end of the tail.

ORCID iDs

G. Lyle Hoffman https://orcid.org/0000-0002-9288-9243
Jayce Dowell https://orcid.org/0000-0003-1407-0141
Martha P. Haynes https://orcid.org/0000-0001-5334-5166

References

Carignan, C., & Purton, C. 1998, ApJ, 506, 125
Chengalur, J. N., Giovanelli, R., & Haynes, M. P. 1995, AJ, 109, 2415
Condon, J. J., Cotton, W. D., Greisen, E. W., et al. 1998, AJ, 115, 1693
Dowell, J. D. 2010, PhD thesis, Indiana Univ.
Giovanelli, R., & Haynes, M. P. 1989, ApJL, 346, L5
Giovanelli, R., Haynes, M. P., Kent, B. R., et al. 2005, AJ, 130, 2598
Haynes, M. P. 2016, The Arecibo Legacy Fast ALFA Survey, http://egg.astro.cornell.edu/alfalfa/data/index.php
Haynes, M. P., Giovanelli, R. I., Kent, B. R., et al. 2018, ApJ, 861, 49, (α.100)
Haynes, M. P., Giovanelli, R. I., Martin, A. M., et al. 2011, AJ, 142, 170, (α.40)
Haynes, M. P., Giovanelli, R. I., & Roberts, M. S. 1979, ApJ, 229, 83
Haynes, M. P., Hogg, D. E., Maddalena, R. J., Roberts, M. S., & van Zee, L. 1998, AJ, 115, 62
Hoffman, G. L., Lu, N. Y., Salpeter, E. E., et al. 1993, AJ, 106, 39
Hoffman, G. L., Lu, N. Y., Salpeter, E. E., & Connell, B. M. 1999, AJ, 117, 811
Hoffman, G. L., Salpeter, E. E., Lamphier, C., & Roos, T. 1992, ApJL, 388, L5
Irwin, J. A., Hoffman, G. L., Spekkens, K., et al. 2009, ApJ, 692, 1447
Jones, M. G., Papastergis, E., Haynes, M. P., & Giovanelli, R. 2016, MNRAS, 457, 4393
Kass, M., Witkin, A., & Terzopoulos, D. 1988, Int. J. Comput. Vis., 1, 321
Koopmann, R. A., Giovanelli, R., Haynes, M. P., et al. 2008, ApJL, 682, L85
Lee-Waddell, K., Spekkens, K., Cuillandre, J.-C., et al. 2014, MNRAS, 443, 3601
Lu, N. Y., Hoffman, G. L., Groff, T., et al. 1993, ApJS, 88, 383
Nilson, P. 1972, Uppsala General Catalog of Galaxies (Uppsala: Uppsala Univ.)
Rots, A. H. 1978, AJ, 83, 219
Saintonge, A. 2007, AJ, 133, 2087
Schneider, S. E. 1985, ApJL, 288, L33
Schneider, S. E. 1989, ApJ, 343, 94
Schneider, S. E., Salpeter, E. E., & Terzian, Y. 1986, AJ, 91, 13
Schneider, S. E., Skrutskie, M. F., Hacking, P. B., et al. 1989, AJ, 97, 666
Serra, P., Westmeier, T., Giese, N., et al. 2015, MNRAS, 448, 1922
Stierwalt, S., Haynes, M. P., Giovanelli, R., et al. 2009, AJ, 138, 338
Wilding, T., Alexander, P., & Green, D. A. 1993, MNRAS, 263, 1075